

Electronic Supplementary Information for **Bimetallic Cyclometalated Iridium Complexes Bridged by a BODIPY Linker**

Gregory D. Sutton, Ku Sun Choung, Karen Marroquin, and Thomas S. Teets*

*Department of Chemistry, University of Houston,
3585 Cullen Blvd. Room 112, Houston, TX 77204-5003, USA
email: tteets@uh.edu*

| <i>Index</i> | <i>Page</i> |
|--|-------------|
| NMR spectra of all new complexes | S2–S14 |
| High resolution mass spectrometric analysis of complexes 3–5 | S15–S17 |
| Additional PL spectra and data summaries | S18–S21 |
| Excitation spectra of 3–5 overlaid with absorption spectrum of 2 | S22–S23 |

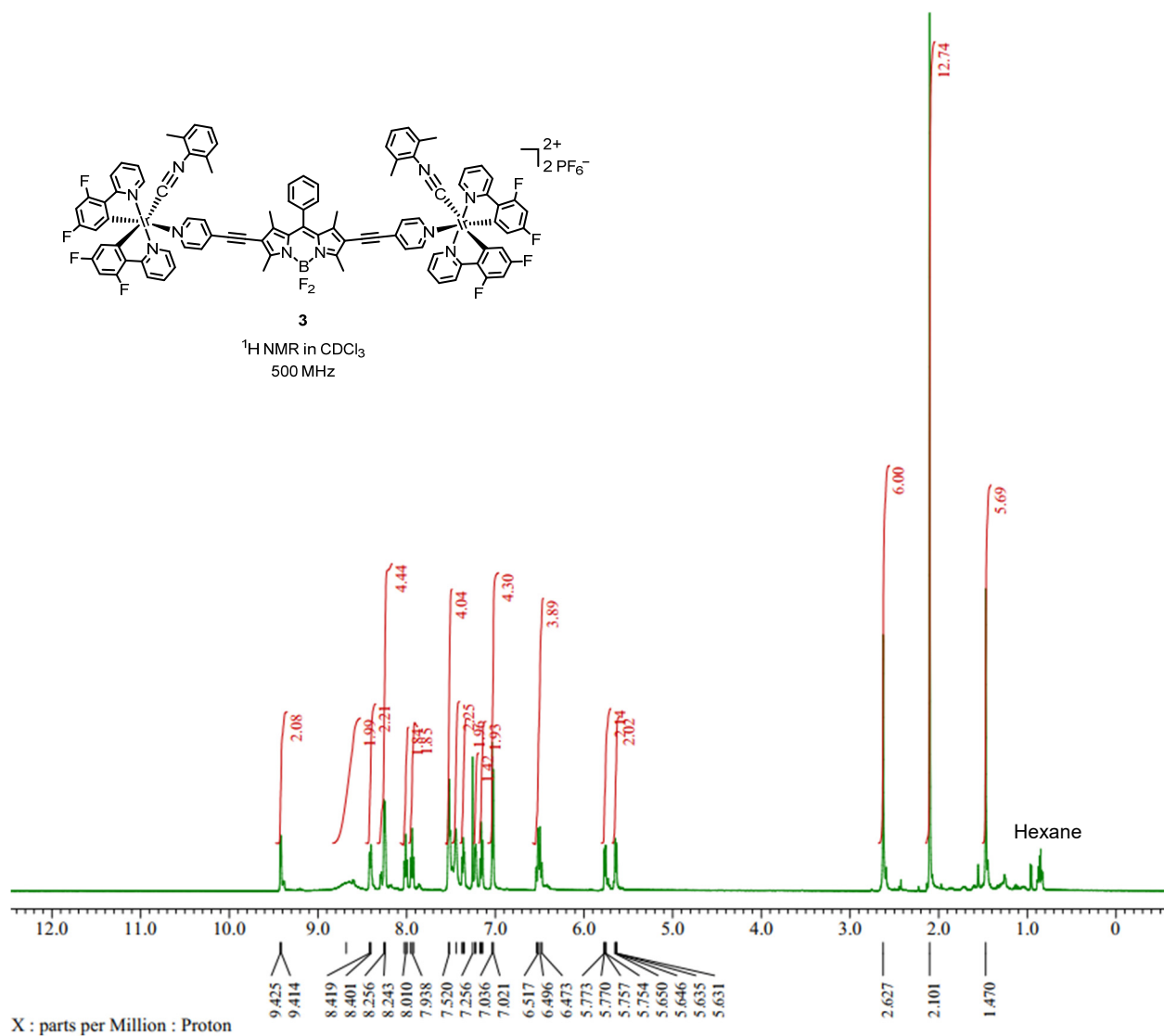


Fig. S1a. ¹H NMR spectrum of complex **3**, recorded at 500 MHz in CDCl₃.

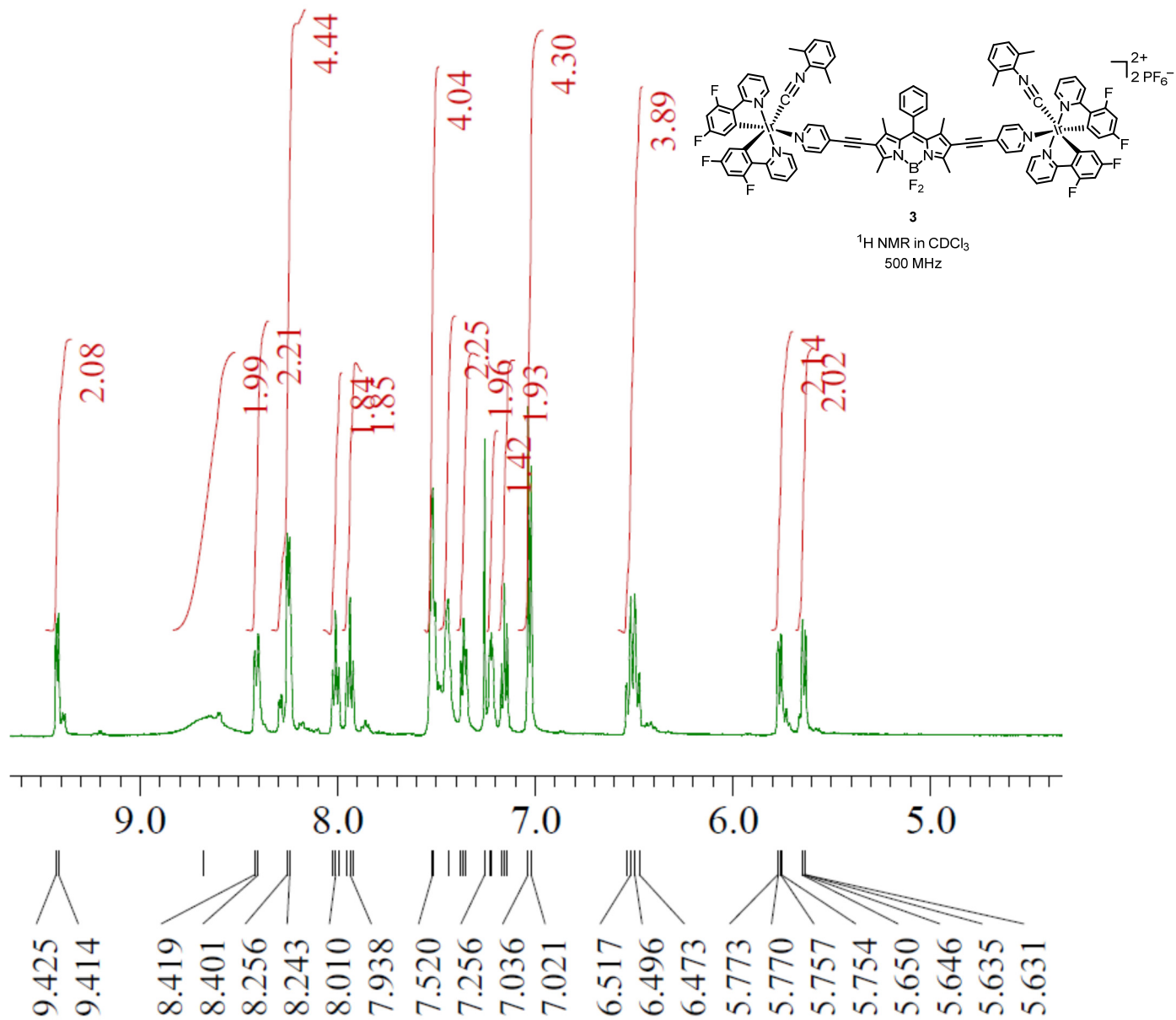


Fig. S1b. Expansion of ^1H NMR spectrum in the aromatic region of complex **3**, recorded at 500 MHz in CDCl_3 .

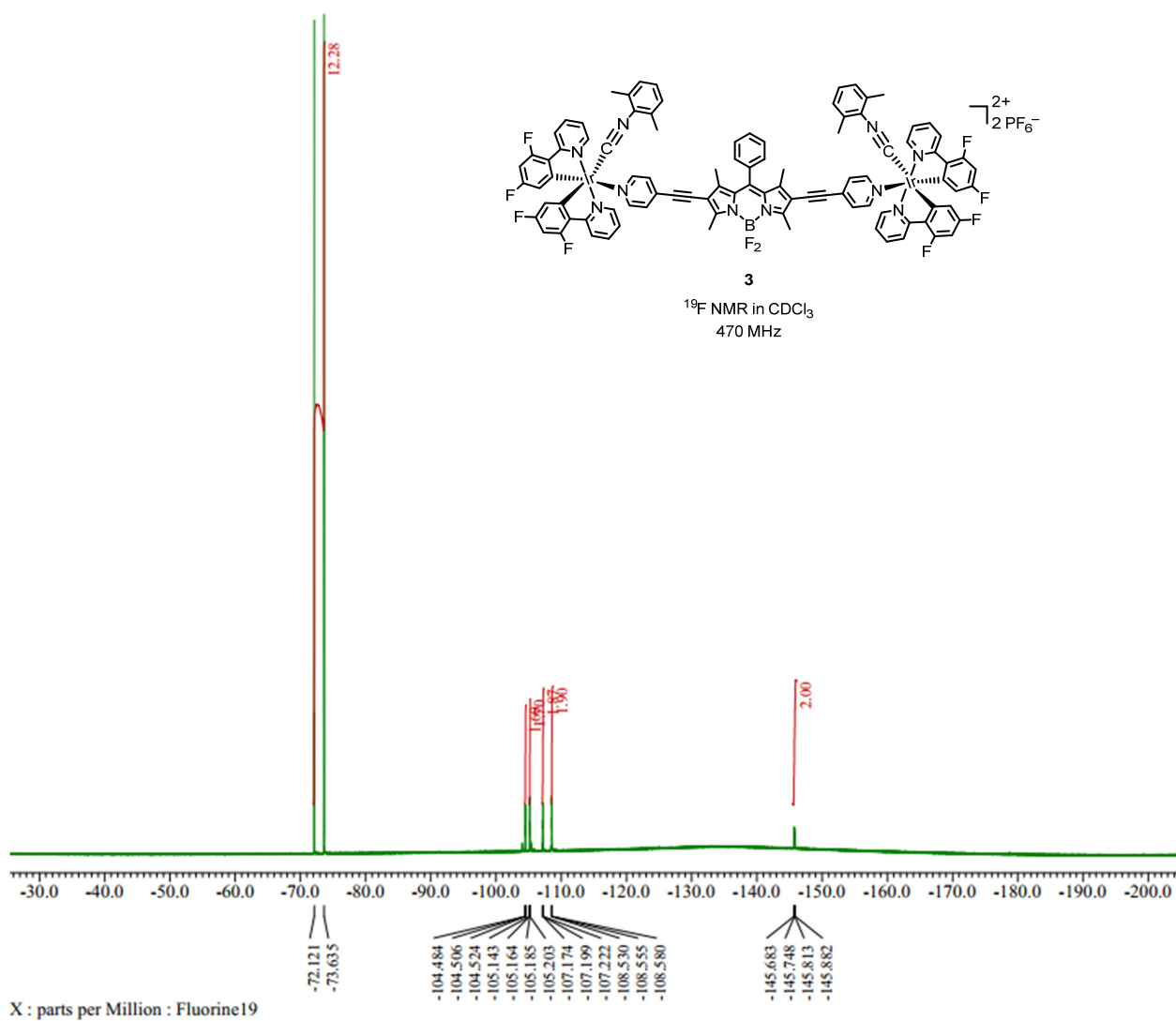


Fig. S2a. ^{19}F NMR spectrum of complex **3**, recorded at 470 MHz in CDCl_3 .

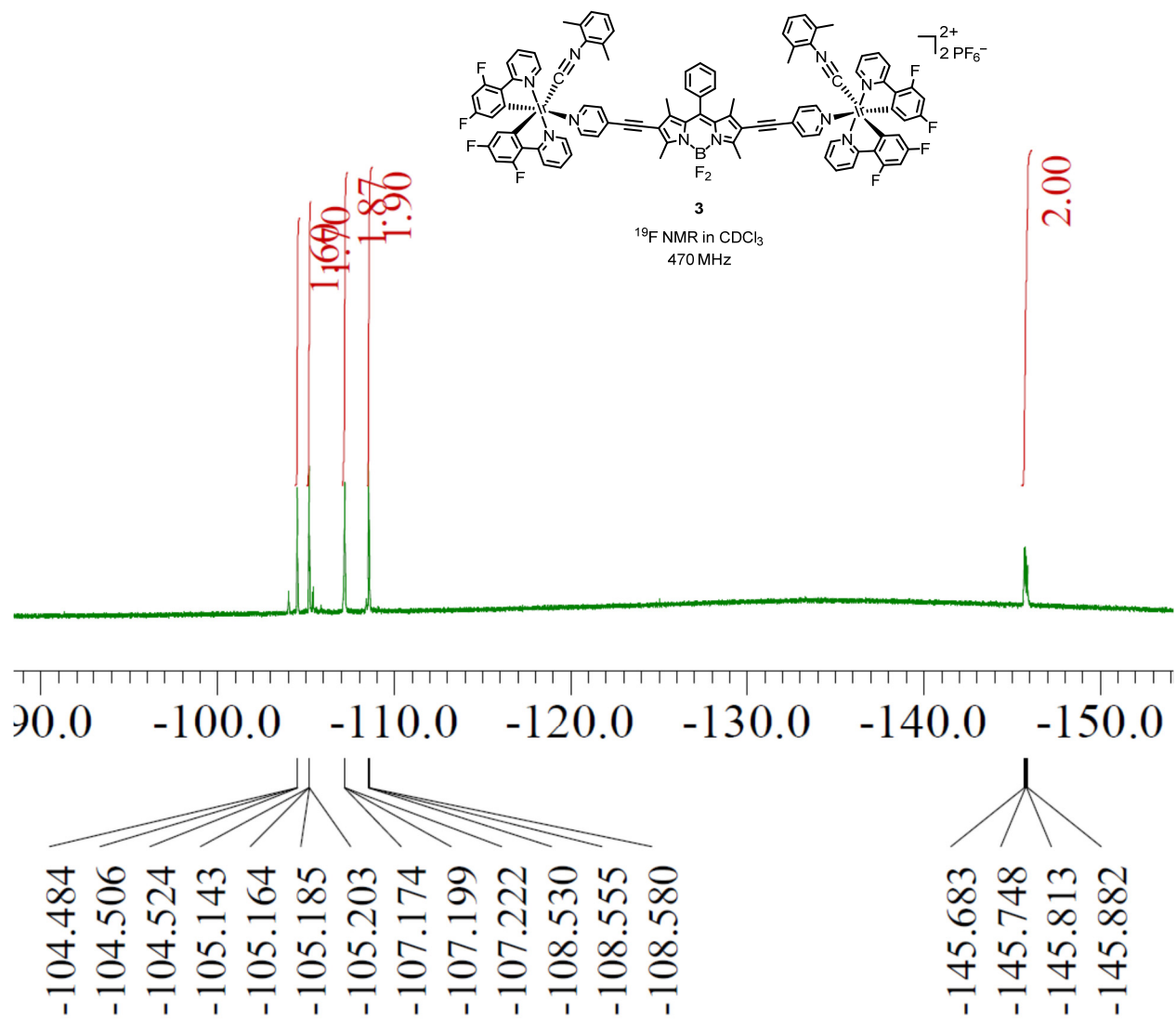


Fig. S2b. Expansion of ^{19}F NMR spectrum of complex **3**, recorded at 470 MHz in CDCl_3 .

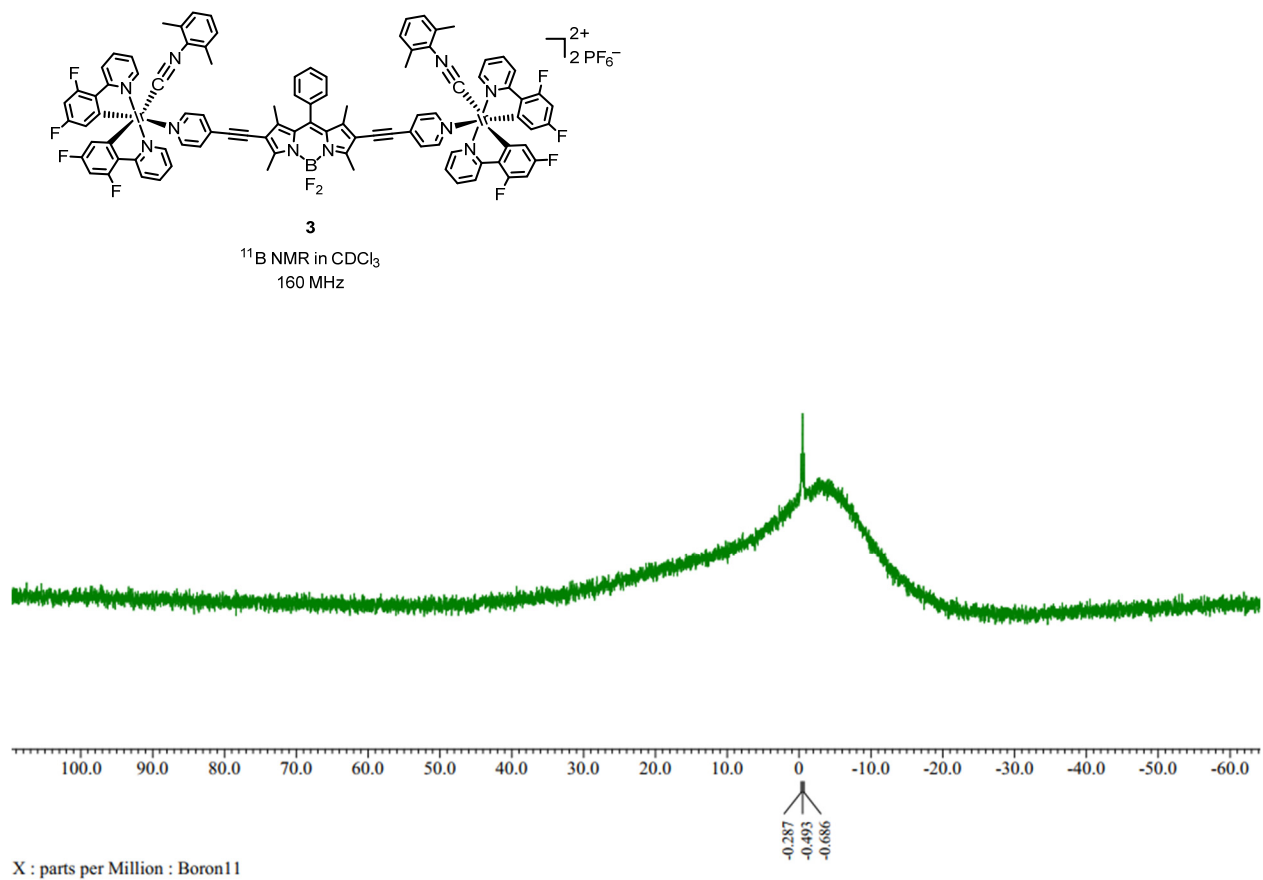


Fig. S3. ¹¹B NMR spectrum of complex **3**, recorded at 160 MHz in CDCl₃.

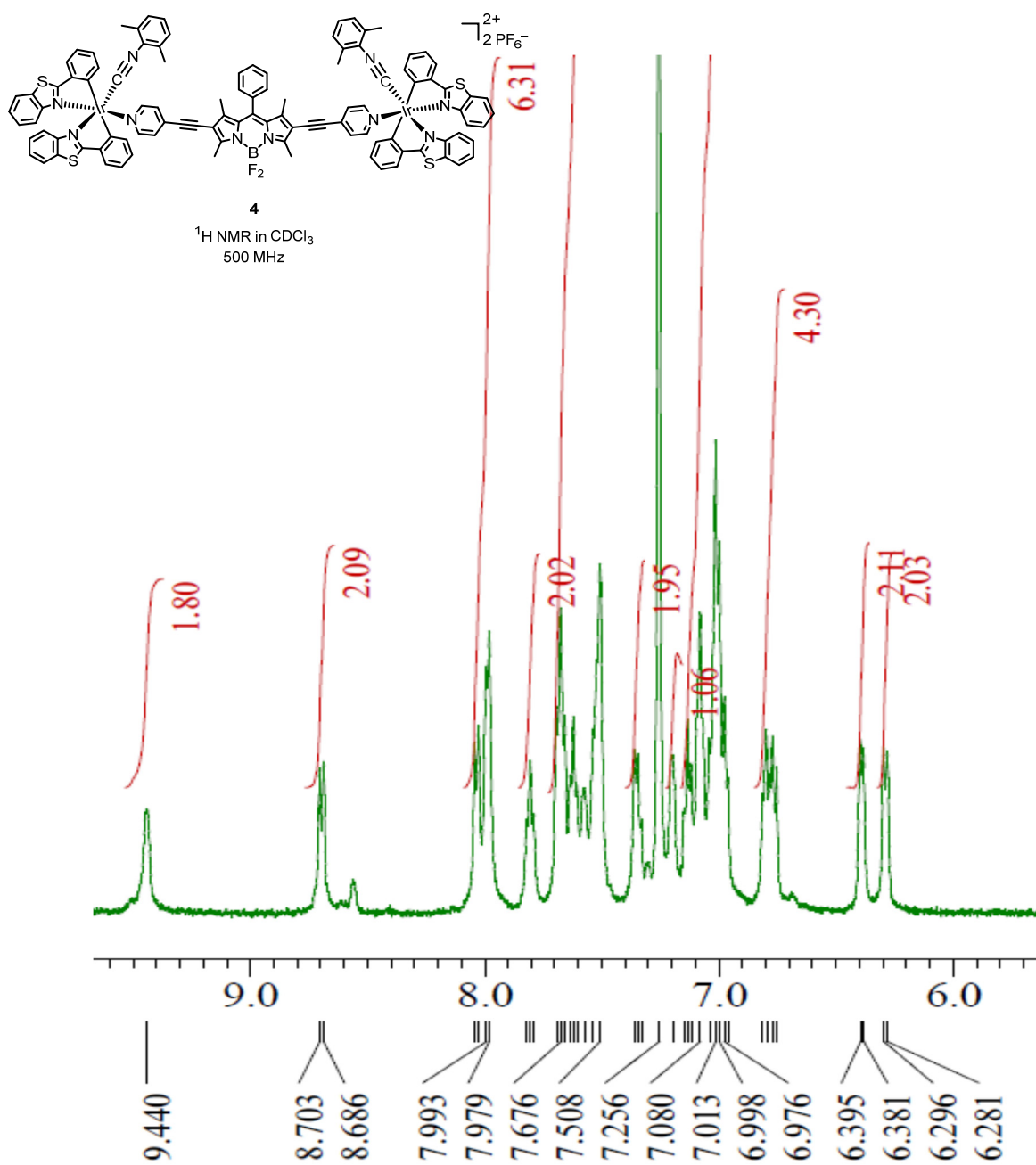


Fig. S4b. Expansion of $^1\text{H NMR}$ spectrum in the aromatic region of complex **4**, recorded at 500 MHz in CDCl_3 .

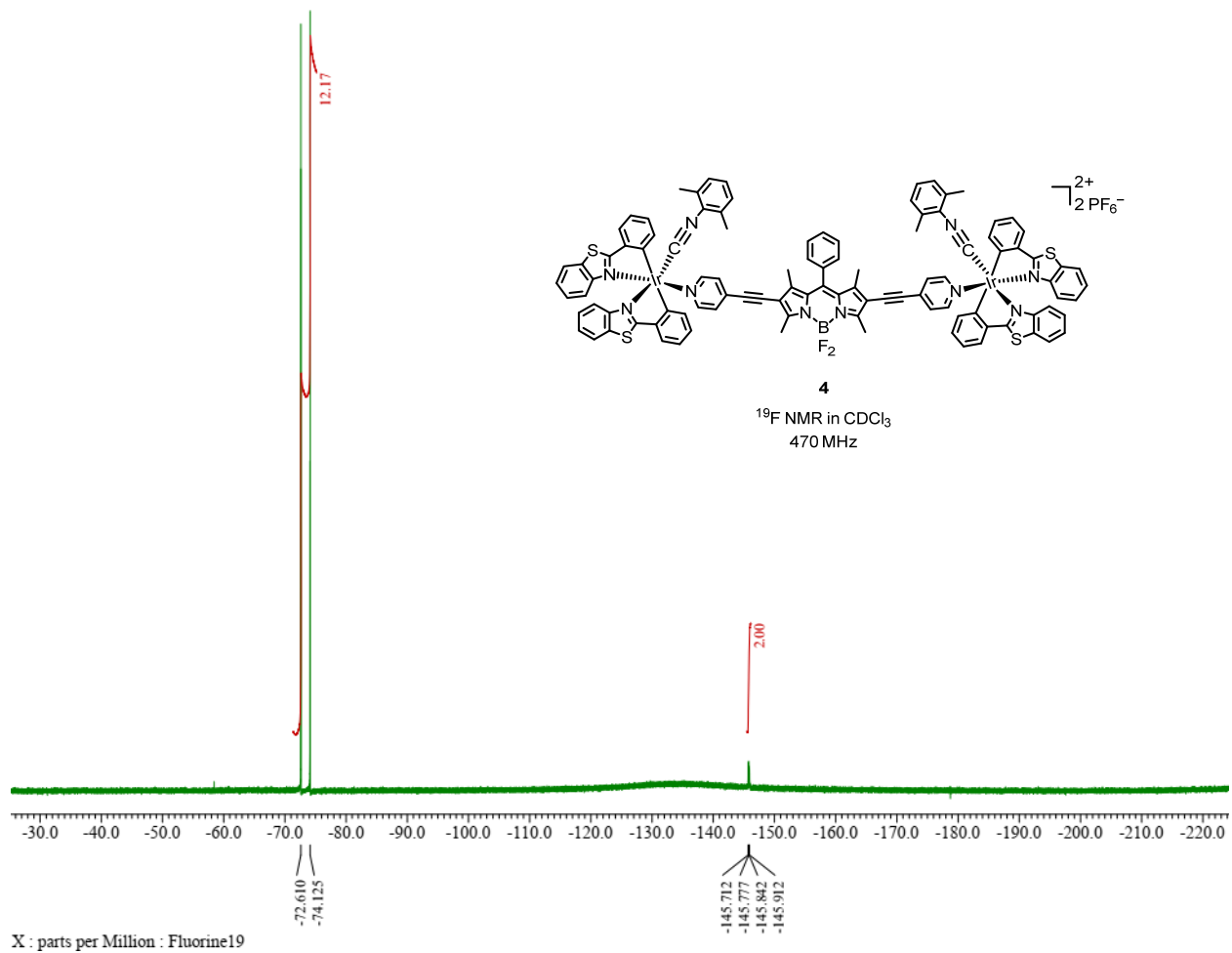


Fig. S5. ^{19}F NMR spectrum of complex **4**, recorded at 470 MHz in CDCl_3 .

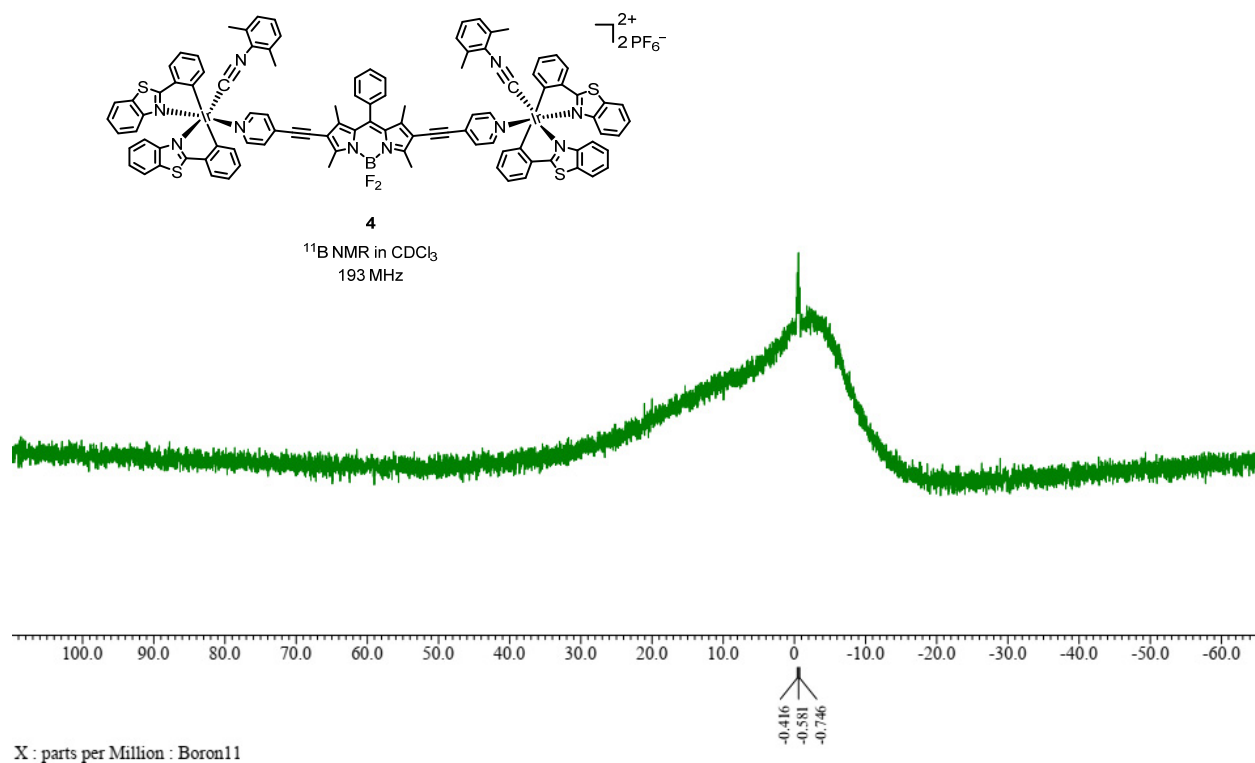


Fig. S6. ^{11}B NMR spectrum of complex **4**, recorded at 193 MHz in CDCl_3 .

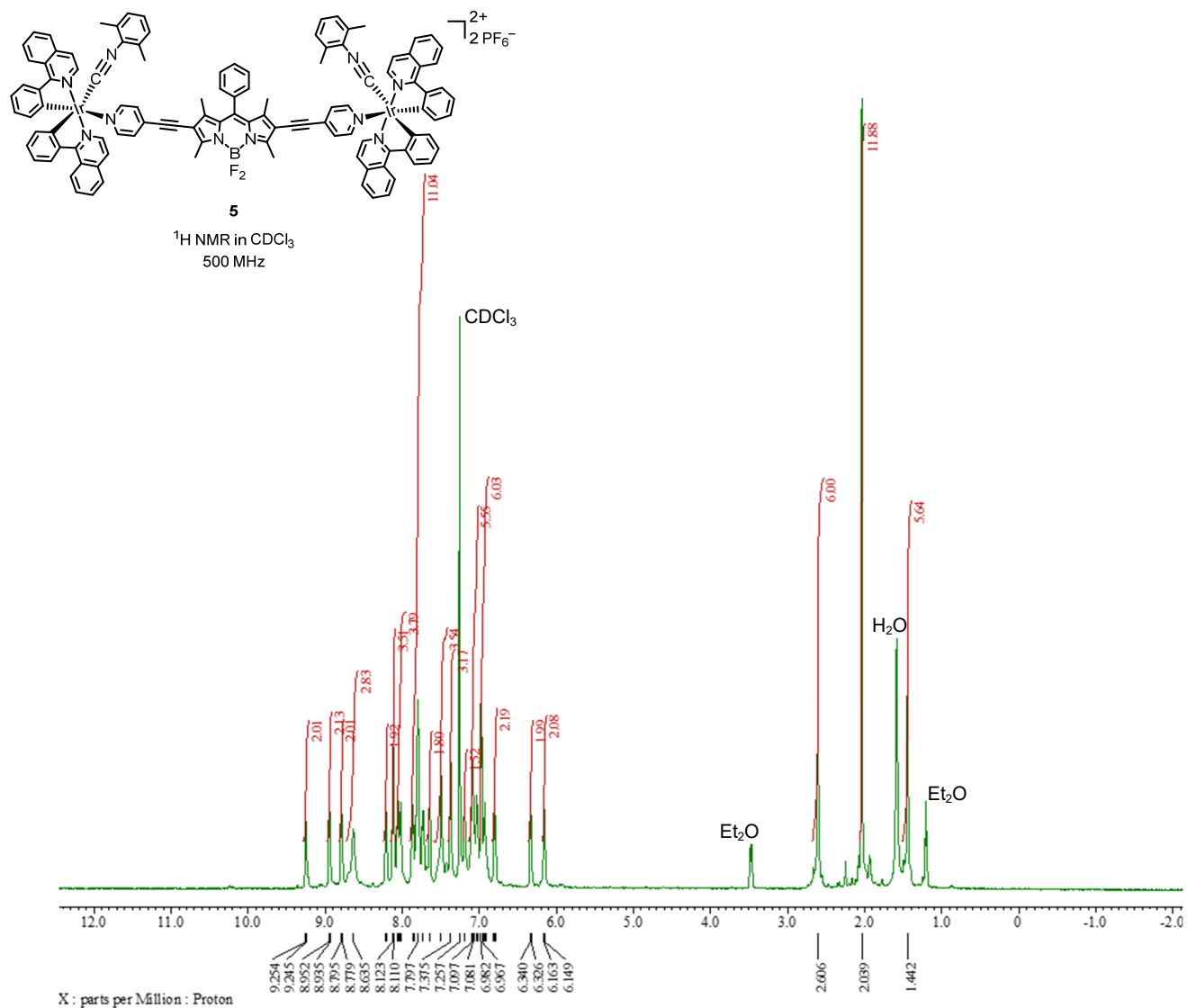


Fig. S7a. 1H NMR spectrum of complex **5**, recorded at 500 MHz in $CDCl_3$.

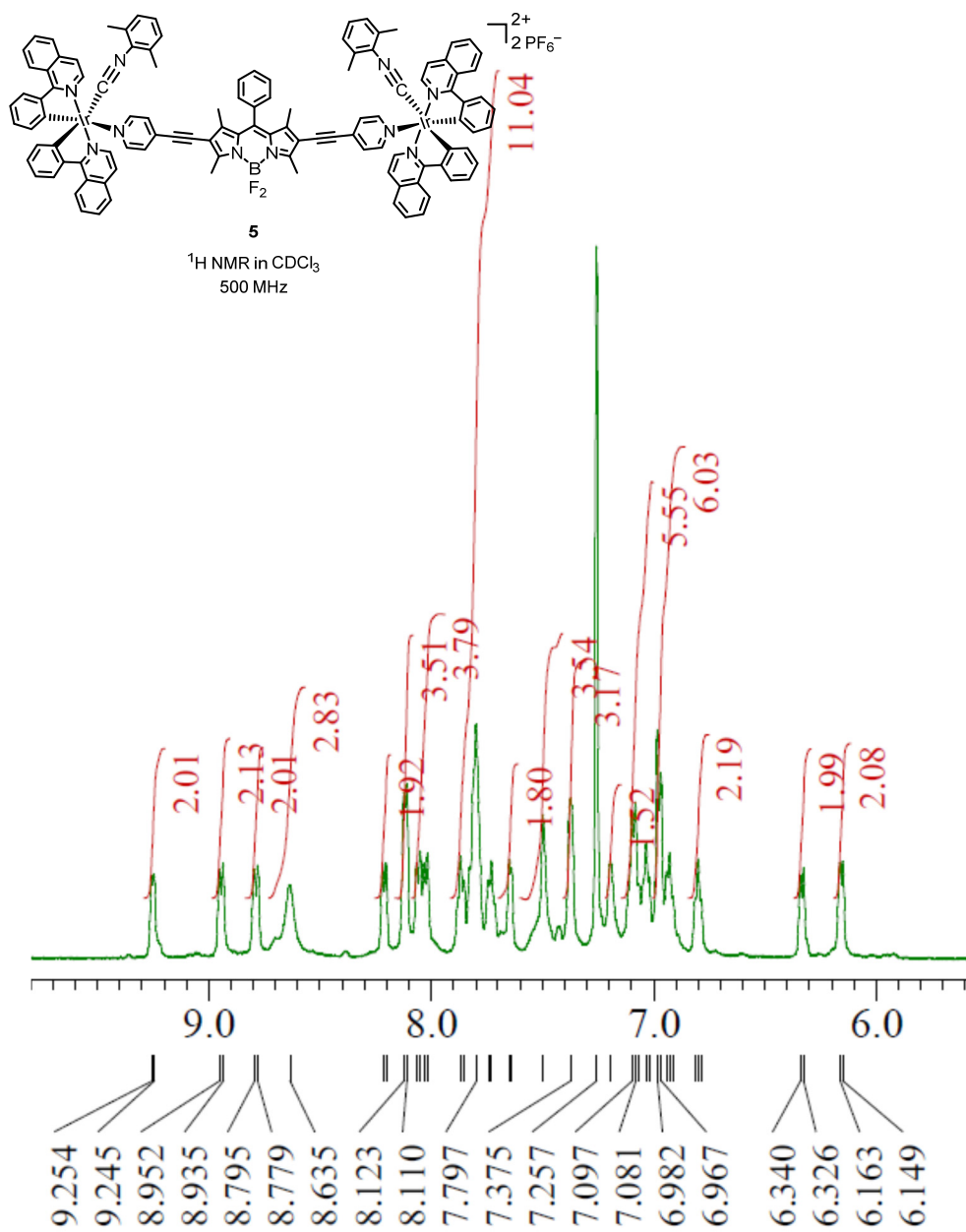


Fig. S7b. Expansion of ¹H NMR spectrum in the aromatic region of complex **5**, recorded at 500 MHz in CDCl₃.

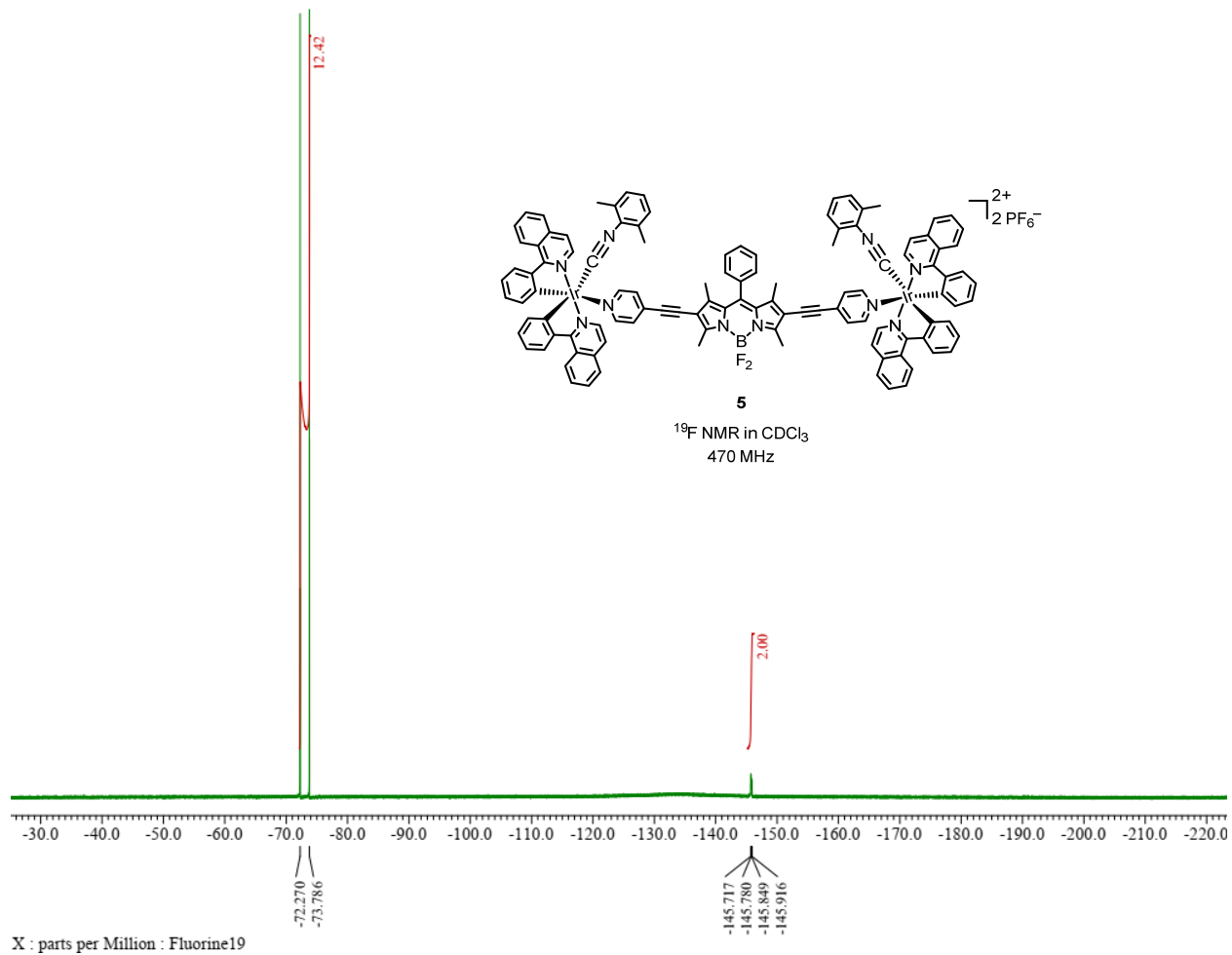


Fig. S8. ^{19}F NMR spectrum of complex **5**, recorded at 470 MHz in CDCl_3 .

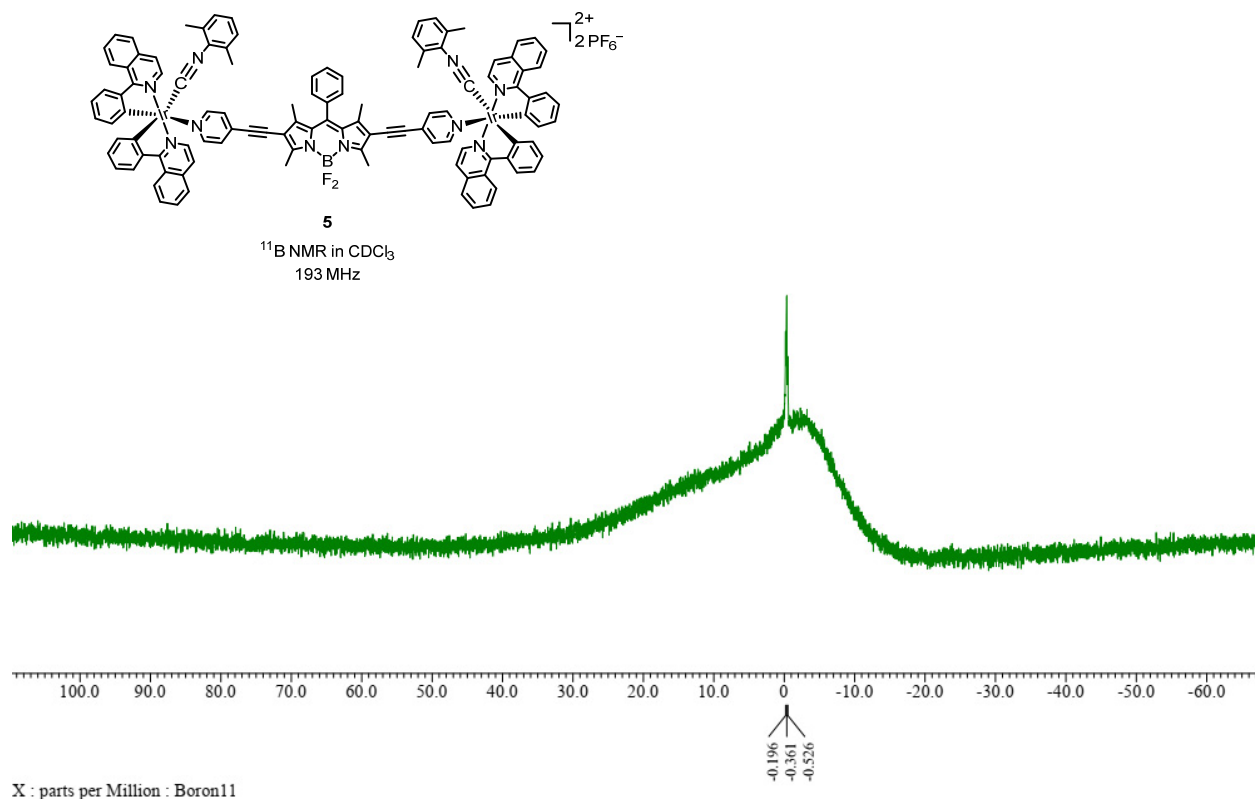


Fig. S9. ^{11}B NMR spectrum of complex **5**, recorded at 193 MHz in CDCl_3 .

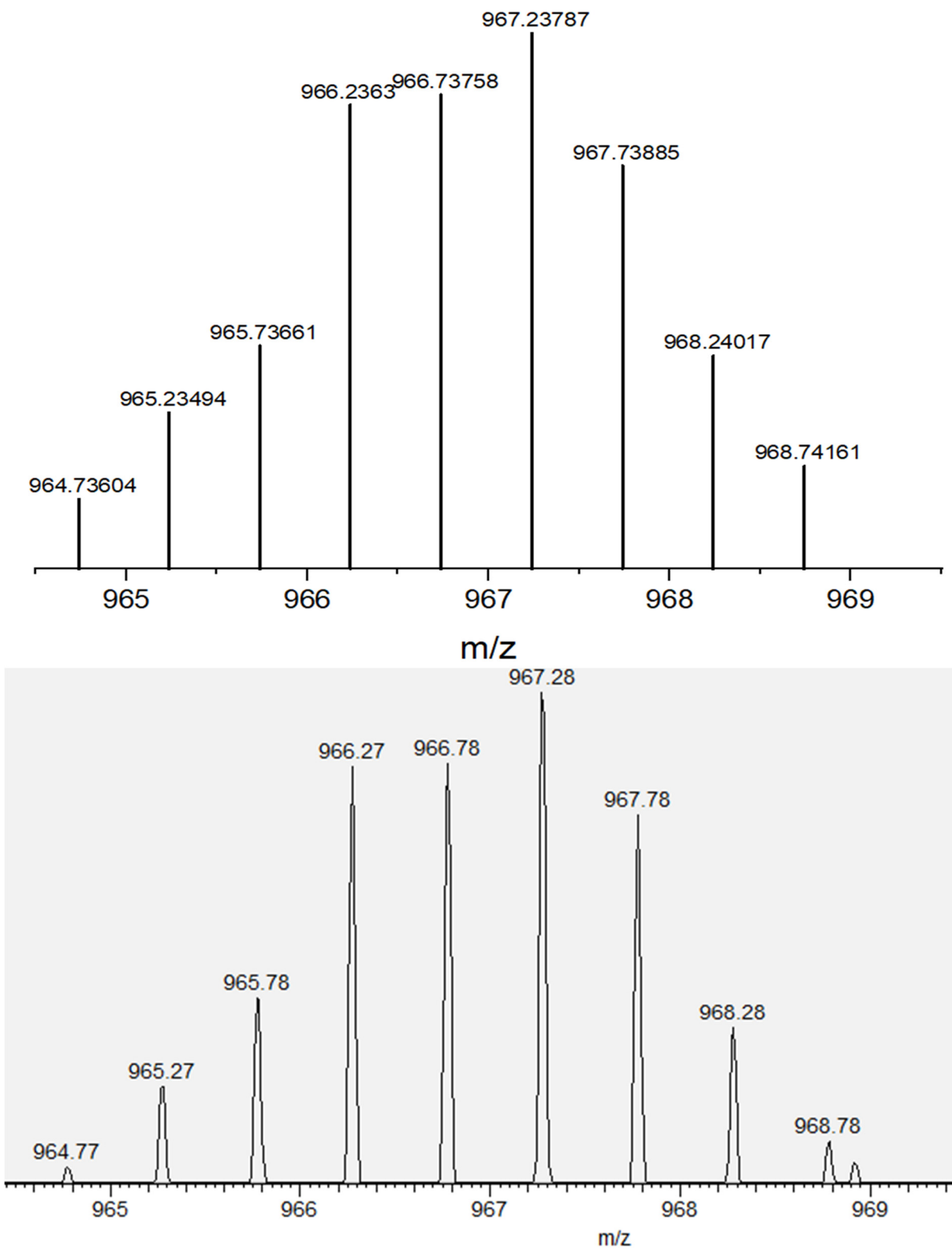


Fig. S10. Simulated (top) and experimental (bottom) ESI-MS data for complex **3**, showing the isotropic distribution pattern for the molecular ion peak ($[M - PF_6]^{2+}$).

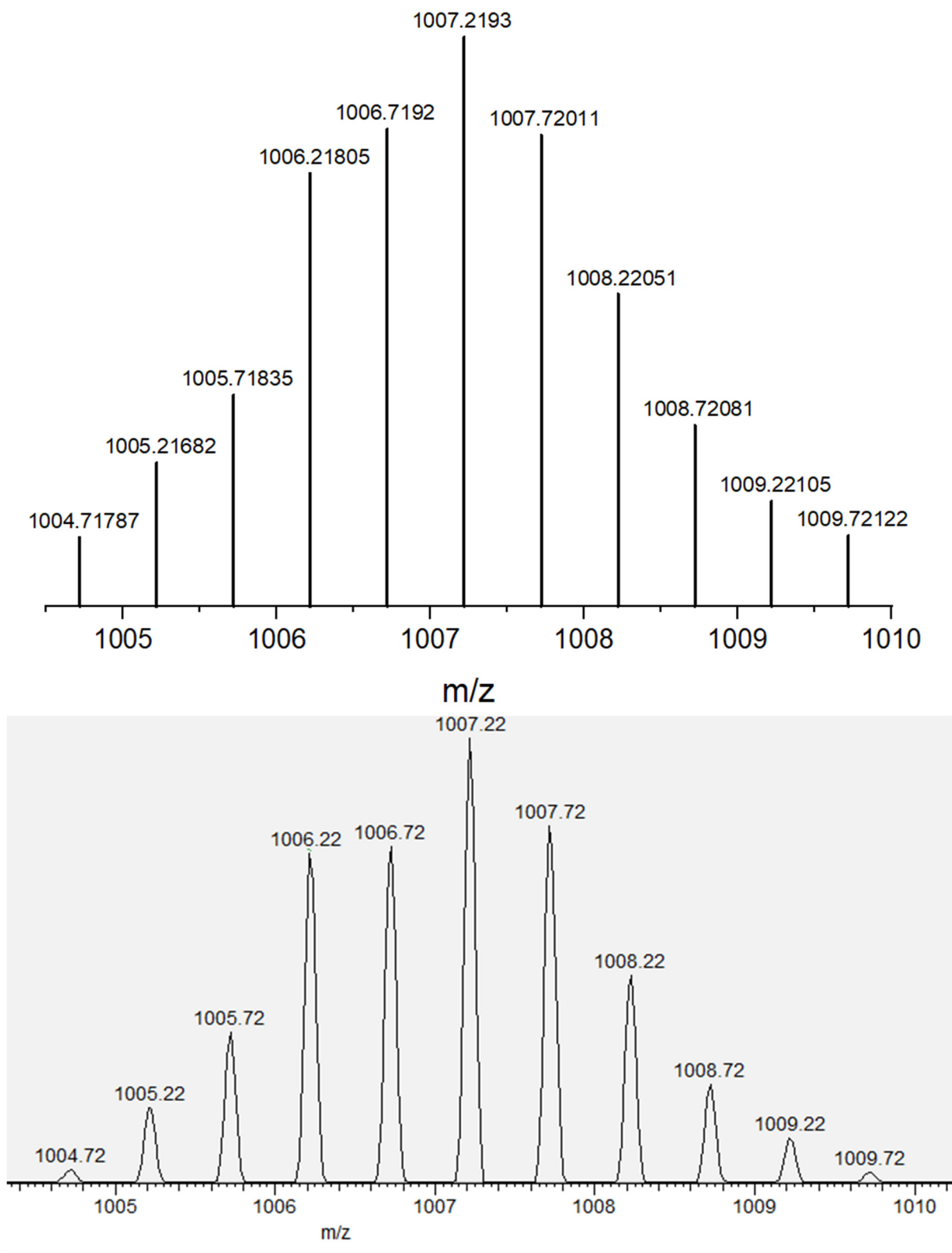


Fig. S11. Simulated (top) and experimental (bottom) ESI-MS data for complex 4, showing the isotropic distribution pattern for the molecular ion peak ($[M - PF_6]^{2+}$).

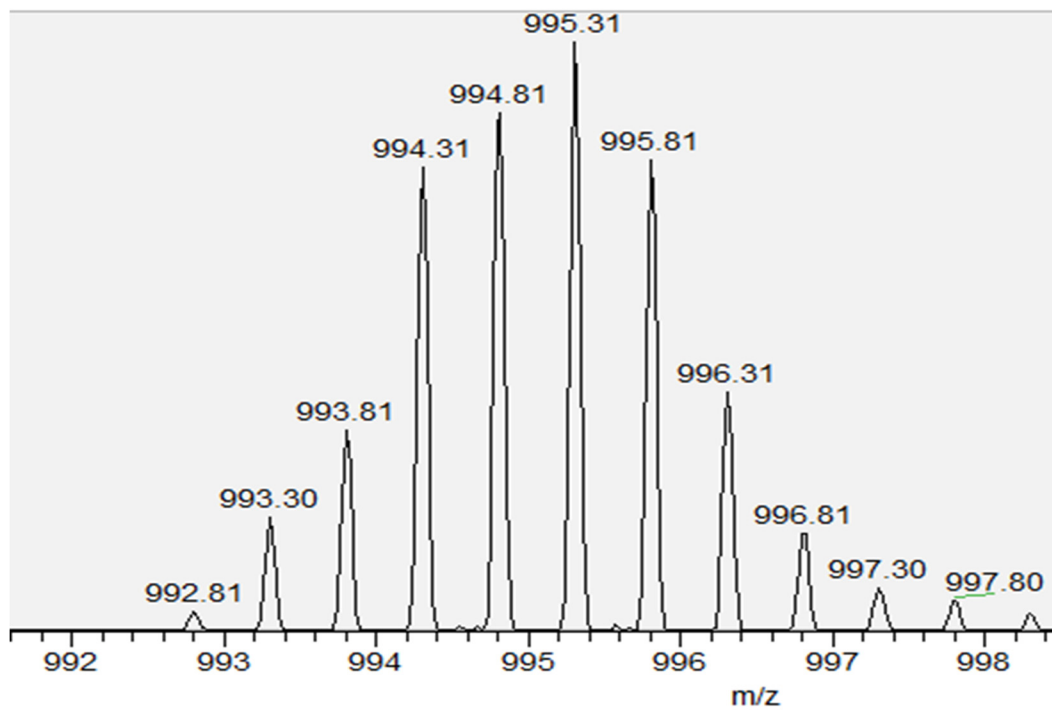
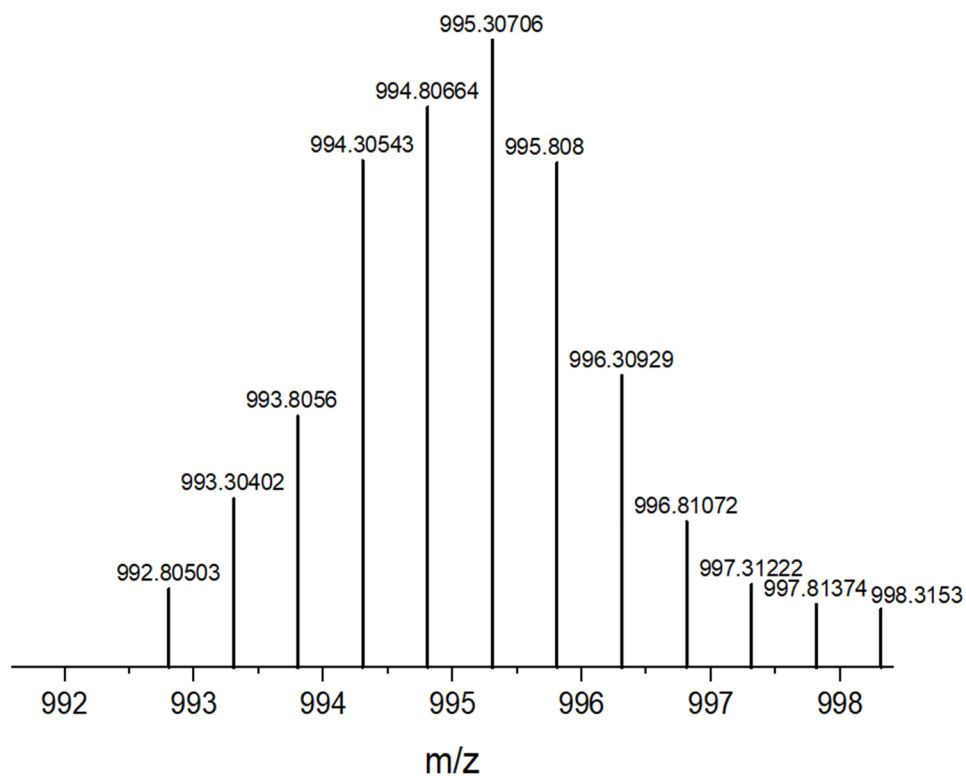


Fig. S12. Simulated (top) and experimental (bottom) ESI-MS data for complex **5**, showing the isotropic distribution pattern for the molecular ion peak ($[M - PF_6]^{2+}$).

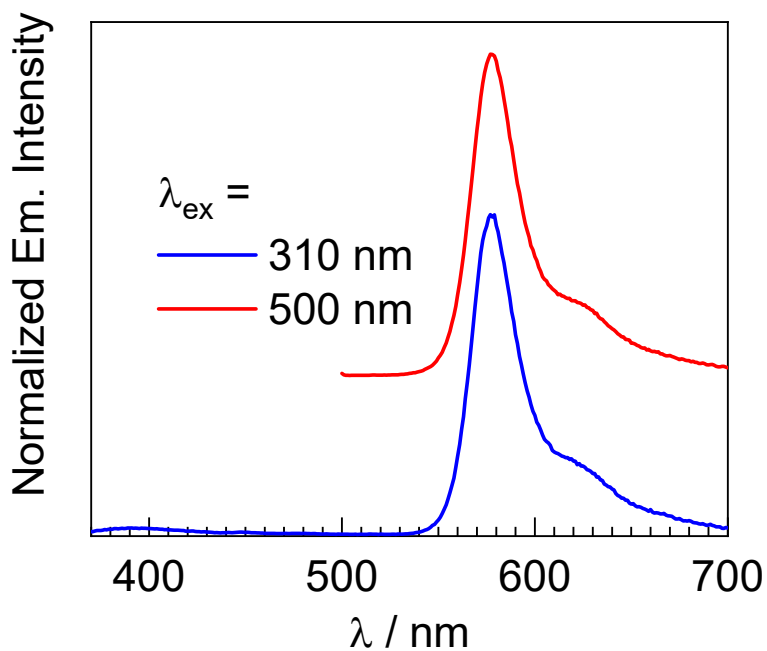


Fig. S13. Overlaid photoluminescence spectra of complex **3** with 310 nm and 500 nm excitation. Spectra were recorded in CH_2Cl_2 at room temperature.

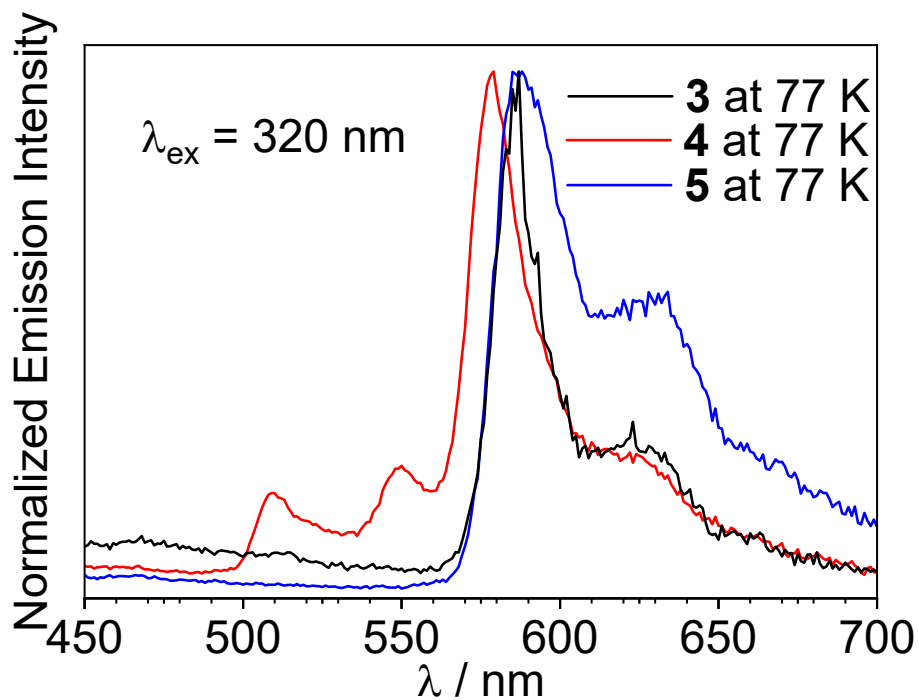


Fig. S14. Overlaid emission spectra of complexes **3** – **5** at 77 K. Spectra were excited at 320 nm and recorded in a 1 : 3 mixture of CH_2Cl_2 : toluene.

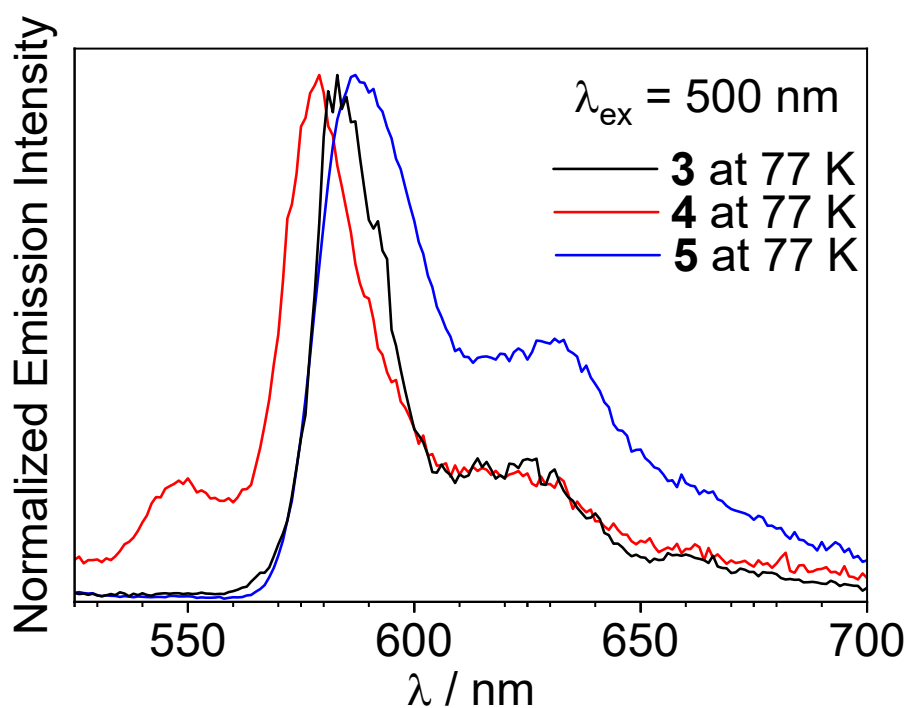


Fig. S15. Overlaid emission spectra of complexes **3** – **5** at 77 K. Spectra were excited at 500 nm and recorded in a 1 : 3 mixture of CH₂Cl₂ : toluene.

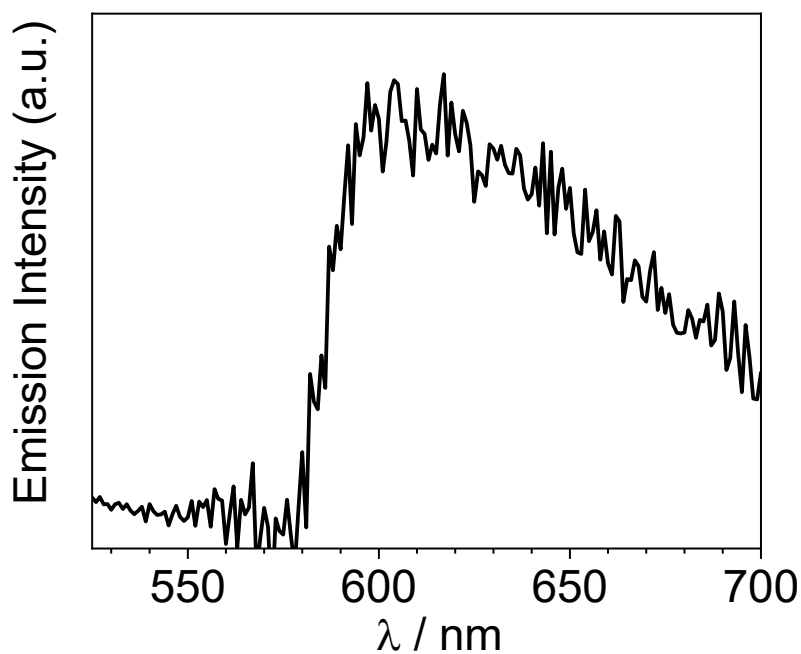


Fig. S16. Difference spectrum of complex **5**, determined by subtracting the PL spectrum obtained with 500 nm excitation from the spectrum obtained with 310 nm excitation..

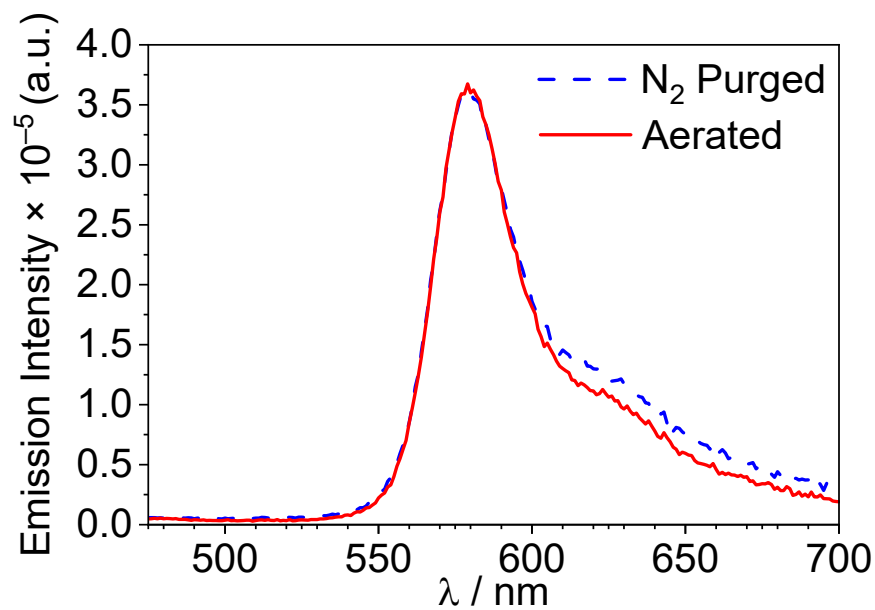


Fig. S17. Emission spectra of complex **5** measured at room temperature in CH_2Cl_2 under N_2 -purged and aerated conditions ($\lambda_{\text{ex}} = 310 \text{ nm}$).

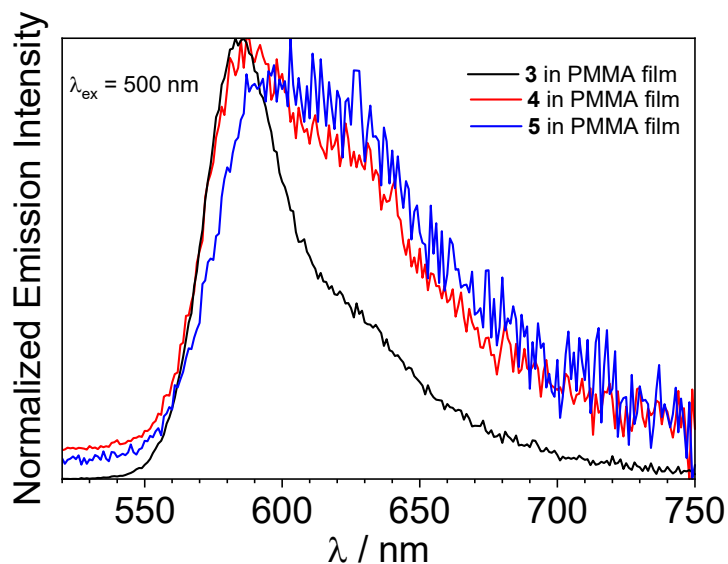


Fig. S18. Overlaid emission spectra of complexes **3** – **5** in PMMA films, doped at 2.5 wt%. Spectra were excited at 500 nm.

Table S1. Summary of emission data ($\lambda_{\text{ex}} = 500$ nm) for Ir-BODIPY constructs **3** – **5** in PMMA films.

| | $\lambda_{\text{em}}/\text{nm}$ | Φ_{PL}^a | τ/ns^b |
|----------|---------------------------------|---------------|--------------------|
| 3 | 583 | 0.87 | 2.8 |
| 4 | 588 | 0.44 | 4.8 |
| 5 | 603 | 0.059 | 13 |

^a Excited at 400 nm. ^b Excited at 455 nm.

Table S2. Summary of emission data ($\lambda_{\text{ex}} = 564$ nm) for Ir-BODIPY constructs **3**–**5** in CH_2Cl_2 solution, along with radiative and nonradiative rate constants.

| | $\lambda_{\text{em}}/\text{nm}$ | Φ_{PL} | τ/ns | $k_r \times 10^{-8}/\text{s}^{-1}$ | $k_{\text{nr}} \times 10^{-8}/\text{s}^{-1}$ |
|----------|---------------------------------|-------------|------------------|------------------------------------|--|
| 2 | 580 | 0.53 | 3.7 | 1.4 | 1.3 |
| 3 | 577 | 0.58 | 3.4 | 1.7 | 1.2 |
| 4 | 579 | 0.87 | 2.6 | 3.3 | 0.50 |
| 5 | 578 | 0.18 | 2.0 | 0.90 | 4.1 |

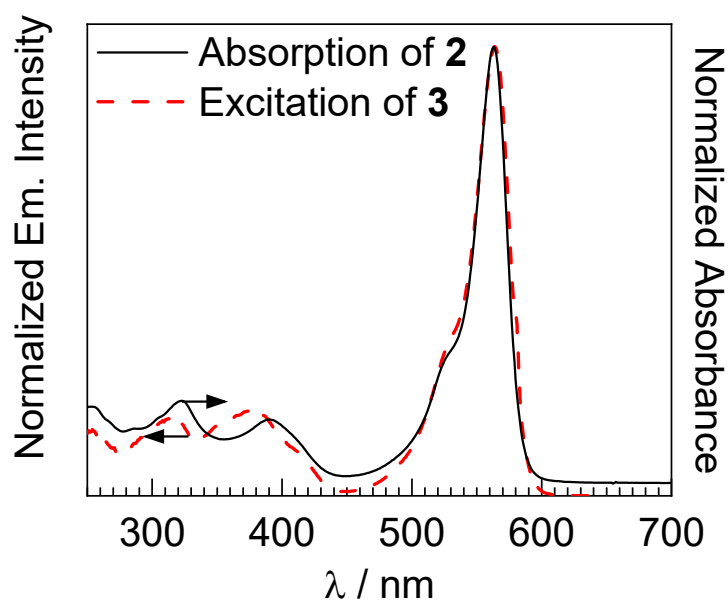


Fig. S19. Overlaid UV-vis absorption spectrum of BODIPY **2** (black solid line) and photoluminescence excitation spectrum of complex **3** (red dashed line). Spectra were recorded in CH_2Cl_2 at room temperature, and for the excitation spectrum $\lambda_{\text{em}} = 564$ nm.

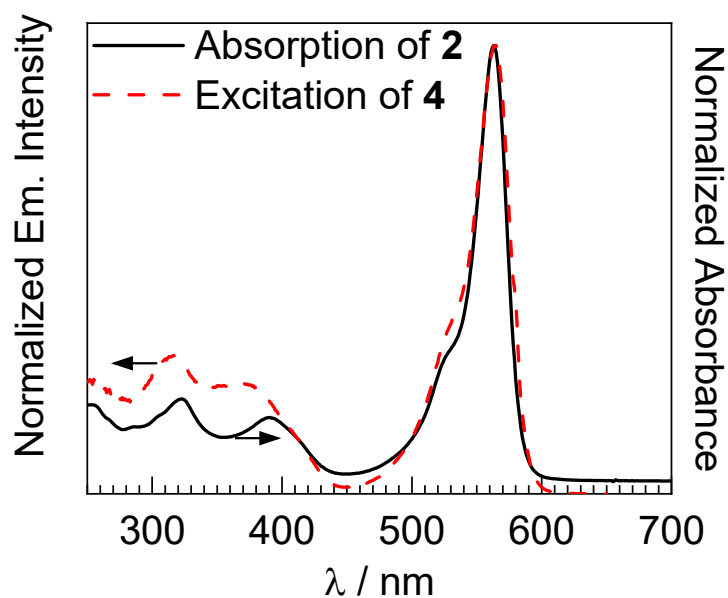


Fig. S20. Overlaid UV-vis absorption spectrum of BODIPY **2** (black solid line) and photoluminescence excitation spectrum of complex **4** (red dashed line). Spectra were recorded in CH_2Cl_2 at room temperature, and for the excitation spectrum $\lambda_{\text{em}} = 564$ nm.

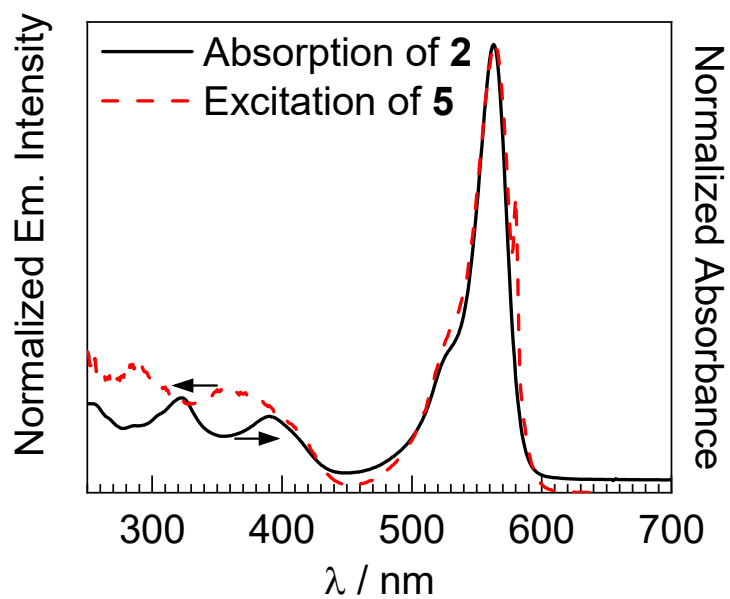


Fig. S21. Overlaid UV-vis absorption spectrum of BODIPY **2** (black solid line) and photoluminescence excitation spectrum of complex **5** (red dashed line). Spectra were recorded in CH_2Cl_2 at room temperature, and for the excitation spectrum $\lambda_{\text{em}} = 564 \text{ nm}$.